12th International Conference on Fracture Mechanics of Concrete and Concrete Structures
FraMCoS-12
B.L.A. Pichler, Ch. Hellmich, P. Preinstorfer (Eds)

https://doi.org/10.21012/FC12.1281
MS02-3:2

IMPACT OF CONCRETE MOISTURE ON THE FATIGUE RESISTANCE OF HIGH-PERFORMANCE CONCRETE UNDER VARIOUS LOAD TYPES

M. MARKERT[*], H. SCHIEWE[*], H. BECKS[†], R. CHUDOBA[†] AND M. CLASSEN[†]

[*] Materials Testing Institute, University of Stuttgart
Pfaffenwaldring 4d, 70569 Stuttgart, Germany
e-mail: martin.markert@mpa.uni-stuttgart.de, www.mpa.uni-stuttgart.de

[†] RWTH Aachen University
Mies-van-der-Rohe-Straße 1, 52074 Aachen
e-mail: hbecks@imb.rwth-aachen.de, www.imb.rwth-aachen.de

Key words: HPC, fatigue behaviour, concrete moisture, uniaxial, triaxial, PTST

Abstract: Currently, the verification of concrete structures exposed to fatigue is very conservative and does not utilise the possibilities of modern concrete mixtures. For this reason, current research projects are focussing on the fatigue properties of high-strength concrete (HPC) and ultra-high-strength concrete (UHPC). Significant influencing factors such as load frequency, load level, composition, and concrete moisture were identified. Several studies have consistently shown that concrete moisture adversely impacts fatigue behaviour across both low and high test frequencies. This detrimental effect becomes significantly more pronounced when specimens heat up during loading. So far, this phenomenon has been most clearly observed under uniaxial loading conditions. The present experimental study aims to investigate the influence of moisture on different types of loading. For this purpose, fatigue tests were carried out under uniaxial, triaxial and combined shear-compression fatigue loading. The latter was introduced using a special test setup, referred to as refined punch-through shear test (PTST). To reduce the influence of temperature, the fatigue tests were conducted at a test frequency of 2 Hz. The confinement level in both the PTST and triaxial tests was set at 20 MPa, while the corresponding lower load level was 5% of the static shear/compressive strength. The upper load level varied between 75% and 95%. Wet and dried concrete were analysed for all three types of loading. The results emphasize the significant impact of moisture on the number of cycles to failure, which varies substantially with the type of loading.

1 INTRODUCTION

With increasingly complex concrete applications, further advancements have become essential, leading to the development of high-performance concretes (HPC). However, the increased use of supplementary materials has introduced new challenges, as the behaviour of these materials remains insufficiently understood. This is particularly evident in the field of fatigue research, where existing conclusions are often highly conservative [1] & [2]. To further develop the potential of concrete as a material and to improve the understanding of its damage behaviour, numerous research activities on the fatigue behaviour of concrete have been initiated in recent years. In the process of these research activities, the moisture content of concrete has been identified as a key parameter that can have a significant influence on fatigue performance [3] & [4]. Beyond moisture, the influence of loading type requires further investigation as well. Although prior studies have addressed this aspect, the limited number of tests and the interplay of variables such as test frequency,

concrete strength and the associated upper stress level have prevented definitive conclusions. Further investigations are therefore necessary. The complexity of triaxial testing has prompted the utilization of the Punch-Through Shear Test (PTST), a method that has demonstrated its effectiveness in various fatigue studies (e.g., [5] & [6]). This method not only simplifies the testing process but also introduces a unique multiaxial loading scenario characterized by shear-compression. The paper presents a detailed analysis of the combined effects of moisture and loading type, focusing on their influence on the number of cycles to failure.

2 MATERIALS AND METHODS

2.1 Material, Geometry and Specimen Preparation

The high-performance concrete (HPC) [7] from the priority programme 2020 (SPP2020) of the German Research Foundation (DFG) was used to investigate the influence of concrete moisture in more detail. A summary of the concrete composition is given in Table 1.

Table 1: Composition of HPC with w/c = 0.35

Component [-]	Density [kg/dm³]	Amount [kg/m³]
CEM I 52,5 R – SR3 (na)	3.094	500
Quartz Sand H33 (0/0.5 mm)	2.70	75
Sand 0/2	2.64	850
Basalt 2/5	3.06	350
Basalt 5/8	3.06	570
BASF MasterGlenium ACE 460	1.05	4.50
BASF MasterMatrix SDC 100 (ST)	1.10	2.85
Water	1.00	176

The water/cement ratio (w/c) was calculated from the amount of cement (500 kg/m³) and water (176 kg/m³) and results in w/c = 0.35. Specimens with a diameter of d = 60 mm and a height of h = 180 mm were produced for the uniaxial and triaxial fatigue tests. After stripping the formwork, the specimens were sawn to the appropriate height and the surfaces were ground plane-parallel.

Specimens with a height of h = 50 mm and a diameter of d = 102 mm were used as PTSTs (Figure 1). The depicted geometry was specifically designed to enable controlled and uniform application of both compressive and shear loading [5]. Radial notches were cut in the outer concrete ring to prevent self-confinement of the concrete specimen. The storage conditions were the same as for the uniaxial and triaxial tests.

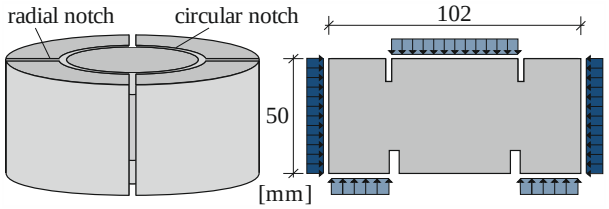

Figure 1: PTST geometry [5]

Two different storage conditions were analysed to describe the effect of moisture. After concreting and stripping, all test specimens from the same batch were stored under water. After 56 days, the specimens from the series D (dry) were dried in an oven at 105 °C. The UW (under water) series specimens were kept under water until testing. The exact storage conditions and resulting moisture contents are summarised in Table 2.

Table 2: Storage condition and concrete moisture of the specimens

Series	Days 1-56	Days 56-Test	Moisture content [%]
D (dry)	under water	105 °C	~0.1
UW (under water)		under water	5.2

The moisture content was controlled by drying the cylinders in an oven at 105 °C for at least 14 days until constant mass. Specimens were weighed before and after drying to determine the water content. For series D, a remaining water content of 0.1% was assumed.

2.2 Test Setup – Uniaxial Fatigue Test

For the uniaxial tests, a 4-column test frame from Form + Test Seidner & Co. GmbH was

used. This test frame is designed for a load of up to 1 MN and is instrumented with a servo-hydraulic cylinder from Schenk. This servo-hydraulic cylinder has a maximum capacity of 630 kN. All of the load tests were performed under force control with a test frequency of 2 Hz. For the triaxial tests (see section 2.3) the test frame had to be adjusted in height. The test frame with built-in cylinder and triaxial cell is shown in Figure 2.

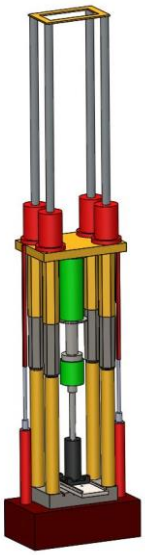

Figure 2: 3D drawing of the experimental setup

In order to compensate for any surface irregularities or deviations from plane-parallelism of the specimens, a ball bearing was added to the load transfer plate. To almost eliminate moisture loss during the test, each specimen was wrapped in a vapour-tight aluminium plastic foil from Brangs and Heinrich (profiTHERM foil) before testing. During the tests, the applied force, the number of load cycles, the deformation of the test specimens and the temperature development were measured constantly. The deformation of the test specimens was measured using three inductive displacement transducers. Type K temperature sensors were used to determine the temperature, which monitored both the surface temperature in the centre of the specimen and the room temperature. The strain was later calculated from the deformation data, assuming a steady strain over the specimen height. A comparable setup is described in [1] & [10].

2.3 Test Setup – Triaxial Fatigue Test

For the triaxial tests, the 4-column test frame from Form + Test Seidner & Co. GmbH was also used (see section 2.2). In addition, a triaxial test chamber type DBTA60-100-RT-Dyn from GL Test Systems GmbH was installed. This test chamber (built in 2008) is designed for operating pressures up to 1000 bar, where the test frequency is limited to 5 Hz and the temperatures up to 50 °C. Very large deformations occurred during the tests, so the test frequency was set at 2 Hz.

The triaxial cell was provided to the MPA University of Stuttgart by the Institute of concrete construction of the Leibniz University of Hannover.

The temperatures were recorded both on the surface of the test specimen and at two points within the triaxial cell using type K temperature sensors. The oil pressure was also measured throughout the tests using an absolute pressure sensor from HBM. This sensor was designed for a pressure of up to 2000 bar.

Three linear displacement transducers (LVDT) were installed to determine the deformations during the testing. To protect the test specimen from the infiltration of oil, it was protected by a custom-fit rubber cover. It was important that the entire measuring system was designed for high oil pressures. As the uniaxial load was limited to a maximum of 630 kN (see section 2.2) and the surface pressure has a major influence on the compressive strength, a surface pressure of 20 MPa was selected. This in return corresponds to an oil pressure of 200 bar. It was maintained constant over the entire duration of the test.

As with the uniaxial tests, a load transfer plate with a cup and ball bearing was used to eliminate possible deviations in the plane-parallelism of the cylinder surface. The triaxial cell including the measurement technology used is shown in Figure 3 and Figure 4.

Figure 3: Triaxial cell used

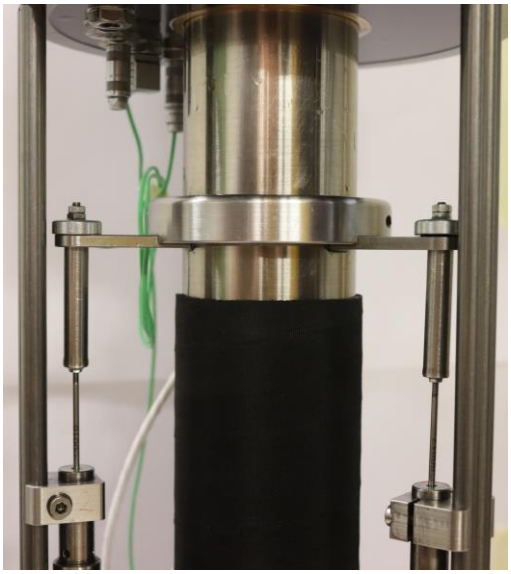

Figure 4: Measurement technology used and internal installation of the triaxial cell

2.4 Test Setup – PTSTs Fatigue Test

To apply an approximately uniform compressive load to the shear surface while visually monitoring deformation and damage behaviour, the test setup shown in Figure 5 – developed and positioned in the laboratory of the Institute of Structural Concrete at RWTH Aachen University – was utilized [5]. The setup is composed of two main components: the lateral compression unit and the shear unit. The lateral compression unit applies compressive force uniformly across the specimen's circumferential surface using four steel jaws, operated by two hydraulic cylinders. To monitor the applied load during testing, two load cells are placed opposite each hydraulic cylinder. The shear unit delivers shear force to the specimen through the main stamp. Full-surface support of the outer concrete ring and load application to the entire inner concrete cylinder ensure an evenly distributed shear stress along the fracture surface while reducing tensile strains induced by bending. To monitor displacement, six LVDTs are mounted at the top and bottom of the specimen. They detect potential tilting of the inner cylinder as well as angular misalignment of the testing surface.

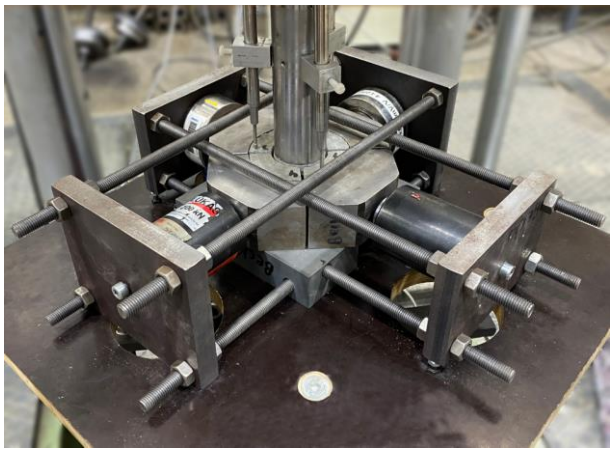

Figure 5: PTST setup [5]

2.5 Experimental Programme

All tests were carried out with a constant test frequency of 2 Hz and a sinusoidal loading, as this frequency was constrained by the limitations of the triaxial test system (see section 2.3). To ensure comparability, all tests (uniaxial, triaxial, and PTST) were conducted at this frequency. The lower stress level was constantly set to $S_u = \sigma_u/f_{c,cyl} = 0.05$ ($S_u = \sigma_u/\tau_{max} = 0.05$ for PTST), while the upper stress level $S_o = \sigma_o/f_{c,cyl}$, ($S_o = \sigma_o/\tau_{max}$ for PTST) was varied according to Table 3, being directly influenced by the static compressive strength $f_{c,cyl}$ (Table 4).
For each of the tests performed, the number of cycles to failure, deformation development and temperature changes were measured. Only the number of cycles to failure is presented in this paper.

Table 3: Experimental programme

Series	S_o	S_u	Test Frequency [Hz]
HPC-D-U	0.75/0.85	0.05	2
HPC-UW-U	0.75/0.85	0.05	2
HPC-D-T	0.75/0.85	0.05	2
HPC-UW-T	0.75/0.85	0.05	2
HPC-D-PTST	0.75/0.85/ 0.95	0.05	2
HPC-UW-PTST	0.75/0.85/ 0.95	0.05	2

3 RESULTS

3.1 Static Compressive/Shear Strength

To calculate the static compressive/shear strength $f_{c,cyl}/\tau_{max}$, measurements were taken on three test specimens for each type of storage and loading. These values served as the basis for determining the standardised upper and lower stresses. The static compressive/shear strengths with the corresponding standard deviations can be found in Table 4.

Table 4: Compressive strengths of the different types of loading and storage conditions

Series	HPC-					
	D-U	UW-U	D-T	UW-T	D-PTST	UW-PTST
Storage condition	D	UW	D	UW	D	UW
Loading type	Uni-axial	Uni-axial	Tri-axial	Tri-axial	shear-com-pression	shear-com-pression
Surface pressure [MPa]	0	0	20	20	20	20
Static compressive/ shear strength $f_{c,cyl}/\tau_{max}$ [MPa]	101.4	90.1	220.0	203.1	76.9	61.2
Standard deviation [MPa]	2.3	3.8	4.0	0.2	2.1	0.6

Based on the results shown in Table 4, it can be assumed that moisture has an influence on the static compressive strength under all types of loading.

In the analysis of the static compressive strengths within each storage type, there are clear differences visible. For example, in dried specimens, the compressive strength under triaxial loading is 117% higher than under uniaxial loading. A similar trend is observed when comparing uniaxial loading to PTST loading. Notably, the compressive strength under triaxial loading at a surface pressure of 20 MPa more than doubles compared to uniaxial loading.
The standard deviation varies widely for all types of loading, with particularly pronounced differences for moist specimens. It is therefore generally difficult to make a suitable statement on the result of the standard deviations.

3.2 Number of cycles to failure

The results of all the tests are summarised in Table 5.

Table 5: number of cycles to failure (mean)

Series		HPC-					
		D-U	UW-U	D-T	UW-T	D-PTST	UW-PTST
Loading type		Uni-axial	Uni-axial	Tri-axial	Tri-axial	shear-com-pression	shear-com-pression
		Number of cycles to failure					
S_o	0.75	16770	1869	25820	2672	96410	3697
	0.85	264	182	7378	368	2514	632
	0.95	-	-	-	-	11	36

Firstly, a comparison is made between the uniaxial and triaxial tests. At the same time, the influence of the moisture content is also taken into consideration. This is followed by PTST results. The result is a comprehensive overview of all types of loading under the additional influence of moisture.

3.2.1 Uniaxial und triaxial tests

The results of the uniaxial and triaxial tests are shown in Figure 6 and Figure 7. In both figures, the number of cycles to failure are compared with the upper stress level on a logarithmic scale. All tests were carried out with a constant lower stress level of $S_u = 0.05$ and a test frequency of 2 Hz.

The results are colour-coded according to their moisture content: In blue (HPC-UW) the specimens which are stored under water and in red (HPC-D) the dried specimens. The different types of loading are represented by different symbols. The uniaxial tests (U) are represented by rectangles (D) and circles (UW) and the triaxial tests (T) by triangles (D) and stars (UW). There is a significant range in the results, mainly due to variations in static compressive strength (Table 4). In particular, the specimens dried at 105 °C before testing show a large scatter. In order to include this scatter in the analysis, the mean number of cycles to failure was calculated for each upper stress level and each test series. The mean values are given in Table 5.

The result of this calculation is plotted in Figure 7. In addition to that, a linear regression function was formed to describe the fatigue behaviour for each test series, which is described by the equation $f = m \cdot \log(N) + b$.

A reference line with values from the Model Code 2010 [11] is also plotted in addition to the four regression lines.

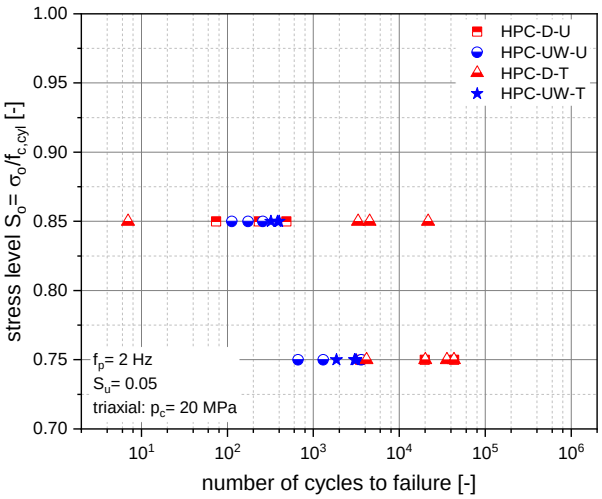

Figure 6: Number of cycles to failure (uniaxial and triaxial)

Figure 7, which depicts the mean values and their regression lines, clearly shows that the lines of the specimens stored under water are parallel to each other. In the case of the dried specimens, the trend lines in the area of higher upper stress levels gap apart. For both the dried and moist specimens, the trend line of the triaxial load (dashed lines) is to the right of the trend line of the uniaxial loads (solid lines). It can be concluded that a triaxial load at the same upper stress level with an external surface pressure of 20 MPa results in a higher number of cycles to failure, regardless of the moisture content. This effect is more evident in the dried specimens, as the two red lines are further apart, especially for an increased upper stress level ($S_o = 0.85$). The moisture content therefore also has a negative effect on the number of cycles to failure, regardless of the type of load.

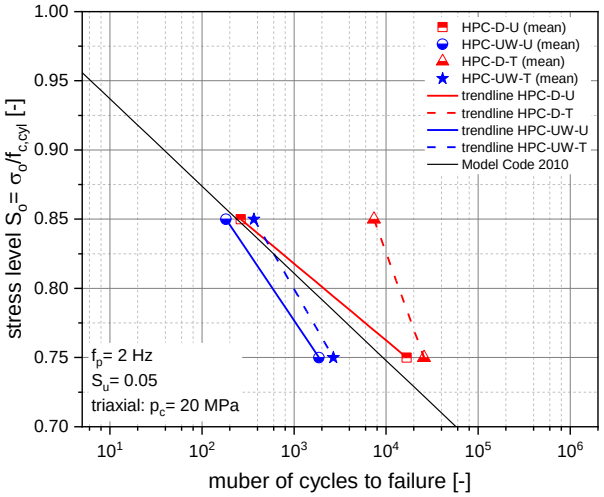

Figure 7: Mean values of the number of cycles to failure and the corresponding trendlines (uniaxial and triaxial)

3.2.2 PTST

Figure 8 illustrates the PTST results, comparing the logarithmic representation of the number of cycles to failure with the corresponding upper stress levels. The testing parameters are summarized in Table 3. The results for moist specimens (HPC-UW-PTST) are represented in blue, while those for dried specimens (HPC-D-PTST) are depicted in red.

Notably, two dry tests at upper stress levels of $S_o = 0.75$ and $S_o = 0.85$ are identified as outliers, marked with an asterisk (*) in the diagram. These tests displayed a significant angular misalignment of the testing surface, leading to an uneven load distribution. The misalignment caused a pronounced stress concentration on one side of the fracture surface, significantly reducing the fatigue life.

An analysis of the angular misalignment across all tests is presented in Figure 9.

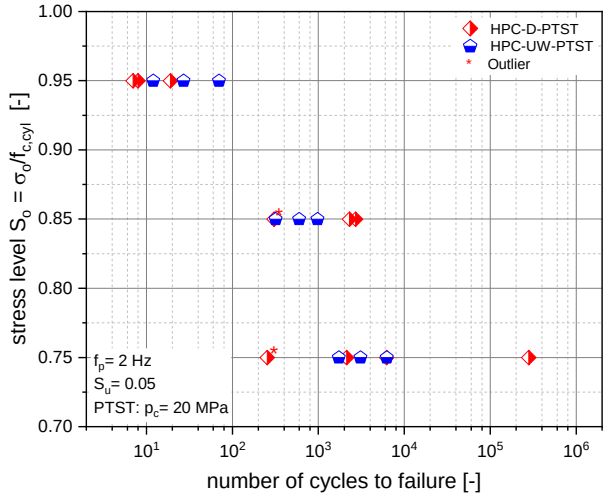

Figure 8: Number of cycles to failure (PTST)

Here, the parameter Δu represents the displacement differential recorded across all six LVDTs. The threshold (dashed line) was determined using the interquartile range method, confirming that the tests are statistically validated outliers.

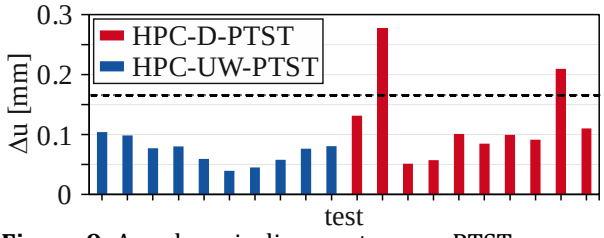

Figure 9: Angular misalignment across PTST

To account for the variability of the static shear strength – which greatly contributes to the observed scatter – the mean number of cycles to failure was calculated for each stress level and test series. The corresponding diagram is shown in Figure 10.

For a better evaluation of the results, regression lines have been added to the diagram. The regression line for the dried specimens is represented by a solid red line, while that for the moist specimens is depicted as a dashed blue line. Outliers were excluded in this process. Notably, the two regression lines intersect at an upper stress level of approximately $S_o = 0.90$. Below this intersection, the dried specimens exhibit significantly higher cycles to failure compared to the moist specimens, whereas above the intersection, the moist specimens outperform the dried ones. This divergence suggests that the detrimental influence of moisture becomes more pronounced as the upper stress level decreases, highlighting the need for further investigation into the underlying mechanisms.

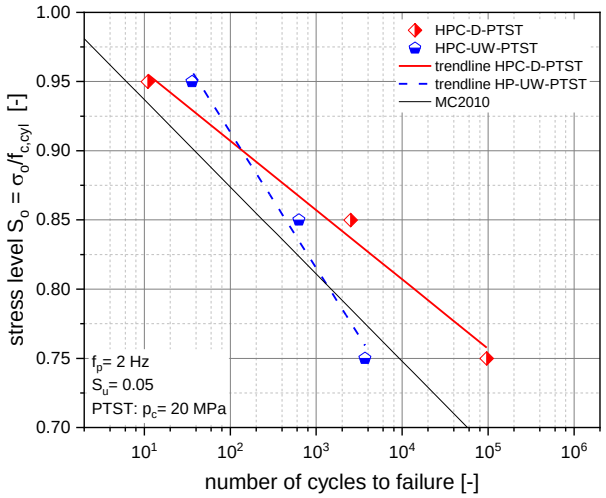

Figure 10: Mean values of the number of cycles to failure and the corresponding trendlines (PTST)

3.2.3 D-Storage condition

Figure 11 summarises the results of all load types with dried concrete. In each of the tests shown, the specimens were dried at 105 °C before the test. The values for the dried specimens under uniaxial loading (HPC-D-U) are represented by solid red lines, while those for triaxial loading (HPC-D-T) are depicted with dashed orange lines. Similarly, the values under shear-compression loading (HPC-D-PTST) are illustrated with dotted purple lines.

For easier visualization, only the regression lines calculated using the mean values of all tests per upper stress level are shown. At first glance, the trend lines for uniaxial loading and shear-compression loading appear nearly parallel. The triaxial load trend line does not follow this pattern. For upper stress levels below $S_o = 0.80$, the values of the triaxial loading lie between the other two types of loading. For upper stress levels above $S_o = 0.80$, the triaxial load tests show a higher number of cycles to failure than the other two

types of loading (uniaxial and shear-compression). In general, it can be said that the fatigue strength of the specimens increases as the upper stress level decreases. In addition, multi-axial loading, both as a triaxial load and with PTST, results in a higher number of cycles to failure than with uniaxial loading.

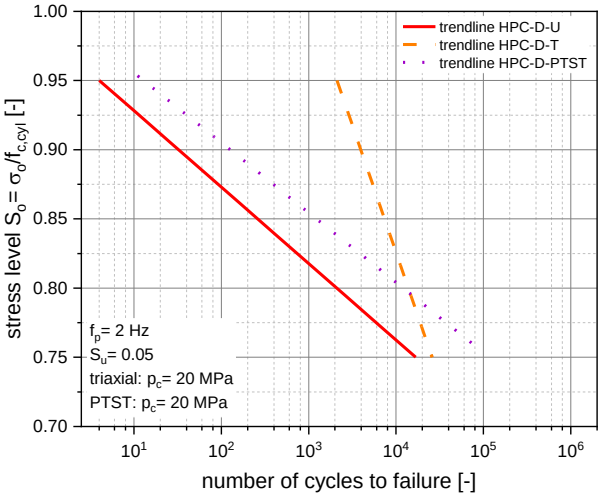

Figure 11: Trendlines with mean values (uniaxial, triaxial and PTST); Dry storage

3.2.4 UW-Storage condition

Finally, the results of the specimens stored under water are analysed. For better visualisation, regression lines were again calculated and illustrated. The different load types are shown in different colours and line types. The trend line of the uniaxial load (HPC-UW-U) is shown as a solid blue line. The trend line of the triaxial tests (HPC-UW-T) is shown in green and as a dashed line and the trend line of the PTSTs (HPC-UW-PTST) is described by a brown dotted line. The results are shown in Figure 12.

The trend lines for the three loading types are nearly parallel, with the uniaxial tests positioned furthest to the left and the PTSTs furthest to the right, while the triaxial load trend line lies in the middle. This behaviour indicates that an increase in surface pressure leads to an increase in number of cycles to failure. The number of cycles to failure also increases as the upper stress level decreases.

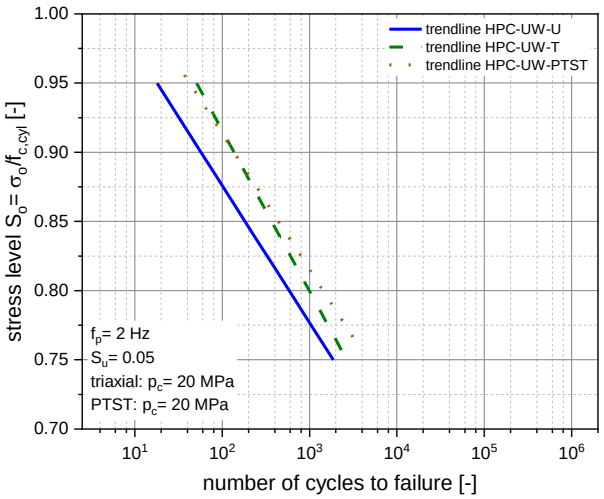

Figure 12: Trendlines with mean values (uniaxial, triaxial and PTST); Underwater storage

4 CONCLUCION AND OUTLOOK

In order to investigate the influence of moisture content and load type on the fatigue behaviour of HPC, tests were carried out with two different concrete moisture contents and three different load types. All tests were performed at a constant test frequency of 2 Hz and a constant lower stress level of $S_u = 0.05$. Regarding the concrete moisture contents, a difference was made between specimens stored under water (HPC-UW) and specimens dried at 105 °C (HPC-D). The tests were performed under uniaxial, triaxial and shear-compression loading. The triaxial loading was applied within a triaxial cell, where a defined surface compression was generated via oil pressure. Shear-compression loading was carried out using Punch-Through Shear Tests (PTSTs), which were conducted within a specially designed testing frame. In both test setups, the surface pressure was set to 20 MPa, while the upper stress level was varied between $S_o = 0.75$ and $S_o = 0.95$ for all load types. Each test was analysed in terms of number of cycles to failure. The results are summarised below:

- Multiaxial loading leads to higher static compressive strengths.
- The dried specimens show higher numbers of cycles to failure for all load types at lower upper stress levels. In the range of higher upper stress levels,

the fatigue performance is higher for the moist specimens.

- The type of loading has a significant influence on the number of cycles to failure. For the same upper stress level, fatigue performance increases with triaxial and shear-compression loading compared to uniaxial loading.
- The increase in number of cycles to failure due to multiaxial loading is much more significant in dry concrete. Although the effect is also visible in moist concrete, it is less evident.

To summarise, it can be concluded that concrete moisture has a significant influence on the number of cycles to failure. Whereby the dried specimens show higher fatigue resistance in the area of low upper stress levels and the moist specimens in the area of higher upper stress levels. This effect could be demonstrated for all load types, uniaxial, triaxial, and shear-compression. In general, the multiaxial load type (triaxial and shear-compression) has a positive influence on fatigue resistance, with a particularly strong influence observed for dried concrete.

ACKNOWLEDGEMENTS

Financial support was provided by the Deutsche Forschungsgemeinschaft (German Research Foundation, DFG) for the projects “Temperature and humidity induced damage processes caused by multi-axial cyclic loading” (project number 353921616) and “Experimental and numerical framework for characterization of high-strength concrete fatigue accounting for local dissipative mechanisms at subcritical load levels” (project number 441550460) as part of the DFG Priority Programme 2020 (SPP2020). This support is gratefully acknowledged. We would also like to thank our colleagues and partners in the SPP2020 for the great discussions. Special thanks go to the Institute for Concrete Structures of the Leibniz University of Hannover for providing the triaxial cell.

REFERENCES

[1] Oneschkow, N., Lohaus, L., 2017. Zum Ermüdungsnachweis von druckschwellbeanspruchtem Beton, Teil 1: Struktur des Ermüdungsnachweises. Beton- und Stahlbetonbau, 112, 530–540.

[2] Oneschkow, N., Lohaus, L., 2017. Zum Ermüdungsnachweis von druckschwellbeanspruchtem Beton, Teil 2: Sicherheitsüberlegungen und Potenzial für Weiterentwicklungen. Beton- und Stahlbetonbau 2017, 112, 611–622.

[3] Markert, M., Birtel, V., Garrecht, H., 2019. Temperature and humidity induced damage progresses in concrete due to pure compressive fatigue loading. In Proceedings of the fib Symposium, Krakow, Poland, 27–29 May 2019; Derkowski, W., Gwozdziewicz, P, Hojdys, Ł, Krajewski, P, Pantak, M, Eds.; FIB: Laussane, Switzerland, 2019; pp. 1928–1935.

[4] Tomann, C., Oneschkow, N., 2019. Influence of moisture content in the microstructure on the fatigue deterioration of high-strength concrete. Struct. Concr. 2019, 20, 1204–1211.

[5] Becks, H., Aguilar, M., Chudoba, R., et al. 2022. Characterization of high-strength concrete under monotonic and fatigue mode II loading with actively controlled level of lateral compression. In: Materials and Structures, Vol. 55, Iss. 252. https://doi.org/10.1617/s11527-022-02087-4.

[6] Becks, H., Classen, M., 2024. New insights into the load sequence effect: Experimental characterization and incremental modeling of plain high-strength concrete under mode II fatigue loading with variable amplitude. In: International Journal of Fatigue, Vol. 185, 108334. https://doi.org/10.1016/j.ijfatigue.2024.108334.

[7] Basaldella, M., Jentsch, M., Oneschkow, N., Markert, M., Lohaus, L., 2022. Compressive Fatigue Investigation on High-Strength and Ultra-High-Strength Concrete within the SPP 2020, Materials 15(11)

[8] Oneschkow, N., Timmermann, T., 2022. Influence of the composition of high-strength concrete and mortar on the compressive fatigue behaviour. Materials and Structures 55, 83. https://doi.org/10.1617/s11527-021-01868-7

[9] Markert, M., Veit, B., Garrecht, H., 2019. “Temperature and humidity induced damage processes in concrete due to pure compressive fatigue loading.” *Proceedings of the fib Symposium*, Krakow, Poland.

[10] Markert, M., Katzmann, J., Birtel, V., Garrecht, H., Steeb, H., 2022. Investigation of the Influence of Moisture Content on Fatigue Behaviour of HPC by Using DMA and XRCT. Materials. 15(1):91. https://doi.org/10.3390/ma15010091

[11] Fib Model Code 2010 (2013) fib Model Code for Concrete Structures 2010. In International Federation of Structural Concrete (Fib); Ernst & Sohn: Lausanne, Switzerland; Berlin, Germany.